Cooperation of human operator and small industrial robot

Borut Povše, Darko Koritnik
R&D department for automation, robotics and electronic instrumentation,
Dax Electronic systems Company, Vreskovo 68, Trbovlje, Slovenia
email: borut.dax@siol.net

Roman Kamnik, *Member*, *IEEE,* Tadej Bajd, *Fellow, IEEE,* Marko Munih, *Member, IEEE*
Laboratory of Robotics and Biomedical Engineering, Faculty of Electrical Engineering,
University of Ljubljana, Tržaška 25, Ljubljana, Slovenia

Abstract
Cooperation between a small industrial robot and human operator is studied in this paper. To ensure safe human-robot interaction several safety features should be introduced into the industrial cell. Despite all the precautions undertaken the collision between robot and man can occur. In present study impact assessments of point robot end-effector with passive mechanical arm were carried out. The impact energy density was calculated and used to evaluate possible injury levels caused by collisions and to determine a safe range of future investigations with human volunteers.

Keywords. Human- Robot cooperation, industrial robot, impact, collision between robot and man

1. Introduction

Future development of industrial production performance and new technologies require coexistence of humans and robotic systems. Future robots will not work behind safety guards with locked doors or light barriers. Instead they will be working in close cooperation with humans which leads to fundamental concern of how to ensure safe physical human robot interaction.

Different approaches have been proposed to study human robot interaction safety (Ikuta, K., 2003), (Heinzmann, J., 2003), (Lim, H., 2000). However, human-robot impacts via crash testing and resulting injuries were to our knowledge mainly investigated by Institute of Robotics and Mechatronics, DLR – German Aerospace Center. Their studies included use of different industrial robots such as Kuka KR3-SI (weight 54 kg), Kuka KR6 (weight 235 kg), Kuka KR500 (weight 2350 kg) and a LWRIII (weight 14kg) light weight robot. The experiments were focused on the chest and head impacts that can cause serious injury or even death. Estimation of injury was made using head injury criteria and compression or viscous criteria for the chest. Injury level was expressed using the abbreviated injury scale, classifying injury severity from 0 (none) to 6 (fatal). The results of the dummy crash-tests indicated that no robot, what ever mass it has, could be life-threatening at end-effector velocity 2 m/s prior to the impact when automobile industry criteria are used and clamping is excluded. Nevertheless, other less dangerous injuries such as fractures of facial and cranial bones can occur already at typical high robot velocities (Haddadin, S., 2007a), (Haddadin, S., 2008a).

When taking clamping of human body in consideration, both head and chest can be severely injured (Haddadin, S., 2008b).

Our research is focused on cooperation of a small industrial robot manipulator and a human worker. Complex assembly is an example of an industrial cell where robot and human can physically interact in order to make the assembly process more efficient and economical. Demanding operations (e.g. insertion of flexible parts) are performed by human worker, while precise assembly of rigid parts is accomplished by a robot.

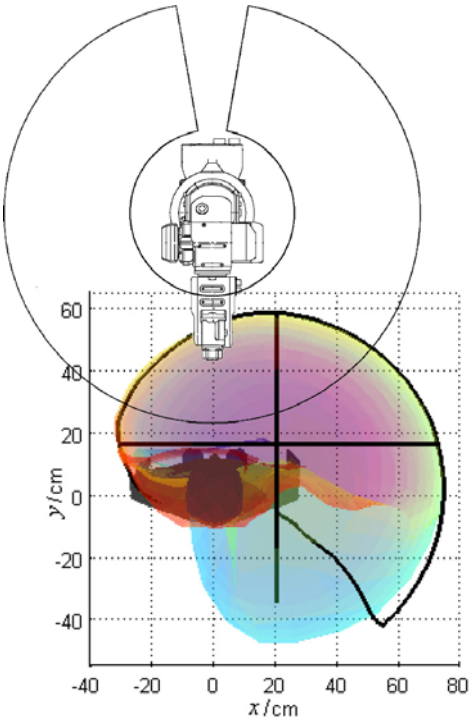

Fig. 1. Common human arm and robot workspace (side view)

We envisage an industrial cell with common human-robot workspace as shown in Fig. 1 (Klopčar, N., 2007). Collision is expected only between robot end-effector and lower arm of human operator. No life-threatening situations can occur; fractures of the lower arm bones are possible in the worst case scenario. The goal is to answer the question whether safe physical human robot interaction is possible when using a small standard industrial robot without human being injured if collision occurs. To ensure safe cooperation, secure end-effector trajectory planning, sensory system (mounted on robot and in the cell) and safety foam rubber clothing (on robot end-effector and human arm) will be introduced into the industrial cell. Nevertheless, the collision between man and robot can occur despite all the precautions undertaken. To study the effect of the impact between robot and a man, a passive mechanical lower arm (PMLA) was developed and equipped with inertial sensors. In the present study impact experiments were carried out with point shaped robot end-effector.

2. Methodology

2.1. Passive mechanical lower arm

In order to get preliminary test results, before starting an investigation with human subjects, a passive mechanical lower arm (PMLA) was built emulating relevant human arm

characteristics. The device consists of a vertical base aluminum pillar to which the arm structure is attached (Fig. 2). The connection between the arm and the base is represented by a passively adjustable shoulder joint. Two smaller aluminum profiles, pneumatic cylinder, and pneumatic rotary unit represent the arm structure. The torque produced by the rotary unit compensates for the gravity, similarly to human biceps muscle and holds the lower arm in horizontal position. The viscoelastic human elbow properties are emulated using a pneumatic cylinder attached to the aluminum profiles representing lower and upper arm. The elbow joint characteristic properties (B– viscous damping, k– elasticity) were determined by adjusting the airflow valves connected to the cylinder.

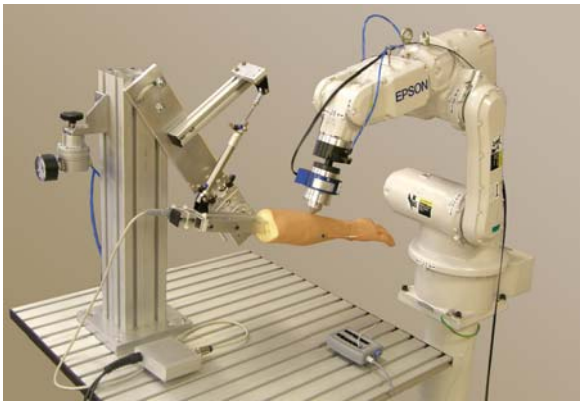

Fig. 2. PMLA and six axis robot with point end-effector

The viscoelastic elbow joint properties are not of significant importance in our current experiments and will be more precisely determined in future studies after completing the experiments with human subjects. The lower arm aluminum structure supports a foam rubber mock-up providing similar elasticity as relaxed muscle tissue. The foam rubber mock-up is covered with silicon esthetic glove resembling human skin. The mechanical lower arm is about the same weight as human lower arm.

2.2. Robot end- effector

Industrial robots are equipped with different grippers and end-effectors according to the task they are performing. In our experiments point shaped robot end-effector was used (Fig. 3) as it appears to be most dangerous in human-robot interactions. With this end-effector we were able to emulate human arm being hit by a conical robot tool.

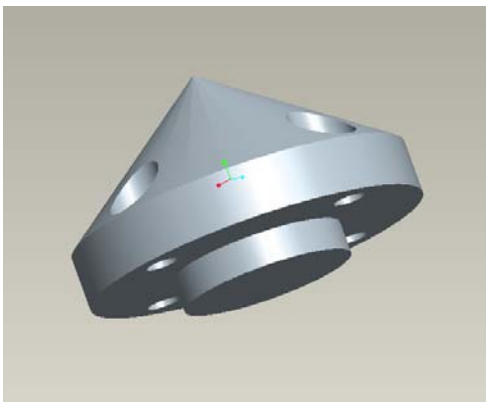
Fig. 3. Robot end-effector for point impact

2.3. Measuring system

The measuring system used in the investigation comprises the inertial sensors incorporating a set of two three-axis accelerometers ADXL203 and three gyroscopes ADXRS150 (Analog Devices, Inc.), three axis force sensor (JR3, Inc.), and the optical kinematic measurement system Optotrak Certus (Northern Digital, Inc.). The inertial sensors were mounted both to the robot end-effector and to the PMLA. The velocities and accelerations were measured at the PMLA supporting aluminum structure and recalculated to the PMLA impact point. The force sensor was installed between the robot's sixth joint and end-effector. The assessed accelerations, velocities, and forces were logged during human-robot impact by a real-time xPC target computer. In addition the robot end-effector and PMLA were equipped with infrared markers. The motion of the robot end-effector and PMLA during the impact was assessed by Optotrak system measuring the motion of infrared measurement markers attached to the objects.

2.4. Impact experiments

In our experiments the robot end-effector collided with the PMLA perpendicularly at constant deceleration. The point of impact was positioned eleven centimeters from the wrist on the dorsal aspect of the lower arm (Fig. 2). The robot end-effector was displaced toward the point of impact along a straight line. Several tests were carried out at different robot decelerations, maximal velocities, and different depths of stop points with regard to the arm surface. The robot end-effector deceleration was changed incrementally from 1000 mm/s^2 to 5000 mm/s^2. The end-effector stop point was located inside the PMLA. The depth from the lower arm surface was changed from 5 mm to 30 mm. After each robot impact, the PMLA was placed into the predefined starting position.

3. Results

3.1. Impact force, PMLA speed, and acceleration

In experiments the robot end-effector was displaced at maximum speed while robot deceleration (acceleration) and the end-effector stop point depth were changed respectively. For example, at robot deceleration set to 1000 mm/s^2 six experiments were carried out with robot end-effector stop point placed from 5 mm to 30 mm (by 5mm steps) inside the PMLA. For each robot deceleration increment of 1000 mm/s^2, all six experiments were repeated. Altogether thirty different experiments were performed. The impact force, PMLA speed, and PMLA acceleration were logged at 8 kHz by the real-time xPC target computer. The measuring results sampled at high frequency give us very good insight into robot end-effector and PMLA impact. The impact forces at maximum robot speed, constant deceleration, and various end-effector stop point depths are shown in Fig. 4. The highest impact force is induced about 30 ms after the start of impact and is highly dependent upon robot end-effector stop point depth. The PMLA speed of impact point is measured using the three-axis gyroscope. The maximal speed is reached about 40 ms after the start of impact and amounts to 0.33 m/s at 30 mm stop point depth (Fig. 5). The corresponding accelerations of the PMLA impact point are shown in Fig. 6.

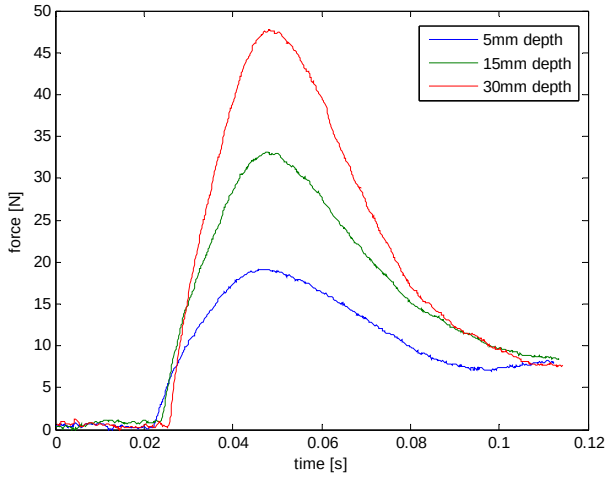

Fig. 4. The contact force during impact at different depths of the stop point

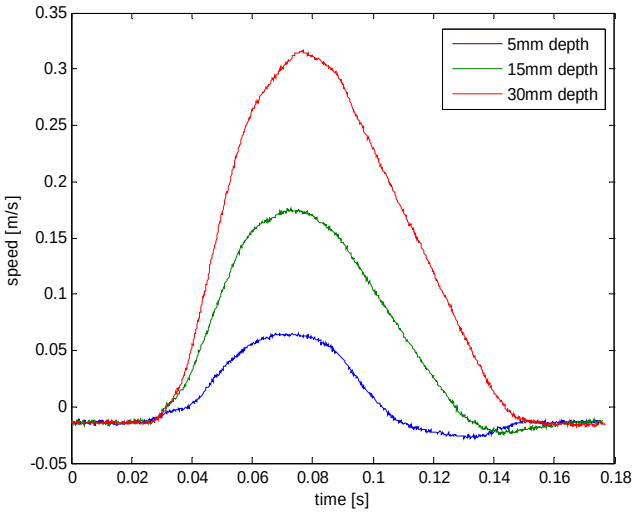

Fig. 5. PMLA speed of impact point

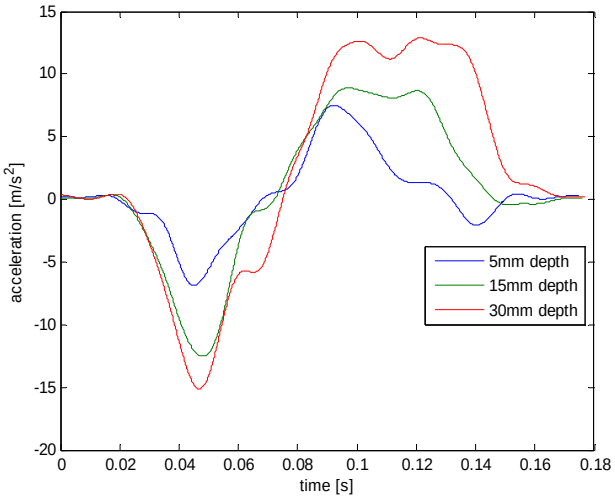

Fig. 6. PMLA acceleration of impact point

3.2. Impact energy density

Although the impact force, PMLA speed, and PMLA deceleration represent useful data for impact studies, they do not provide information regarding the degree of possible injury one would suffer from the impact. The injury intensities for the point impact can be evaluated by calculating the impact energy density. Higher impact energy density causes higher injury level (Haddadin, S., 2007b) and is calculated as

$$e_A = \frac{\int_{s_{impact\_start}}^{s_{impact\_stop}} F \cdot ds}{A_{end-effector}}. \quad (1)$$

In Eq. 1 F is the impact force applied to PMLA; s_{impact_start} and s_{impact_stop} are the distances between the robot end-effector and the center of the lower arm (supporting aluminum rod of the PMLA) at the start and at the end of impact, while $A_{end\text{-}effector}$ is the contact surface area between the robot end-effector and the PMLA. The effective contact surface area used in the calculations was measured using a stamp method. The end-effector was dipped into ink and pressed onto the PMLA. Afterwards, the imprint surface was measured. During impact the robot end-effector kinetic energy is transferred to the lower arm tissue (foam for the PMLA) only from the point where the end-effector touches the lower arm (s_{impact_start}) to the point where the distance between the end-effector and the lower arm center is the smallest (s_{impact_stop}). After that point the robot end-effecor kinetic energy is transferred to the PMLA kinetic energy since the robot end-effector starts to push the lower arm. The energy received by the tissue divided by the contact surface area is the energy density, Eq. 1. However, the energy density can only be used to evaluate contusions expressed by bruises and crushes (Haddadin, S., 2008c). Abrasions, laceration, and stab wounds have to be investigated using different criteria and are not likely to occur during impact with the end-effectors used in our investigation. The point end-effector has 0.04 cm^2 contact surface area and is not considered to be a sharp robot tool that can penetrate human skin at the forces and velocities evaluated in our experiments. In most cases robot tool sharp edges and corners can be avoided or covered with round shaped material when constructing the end-effector.

Tab. 1. The energy density [J/cm^2] during point impact

Stop point depth [mm] \ Robot acceleration [mm/s^2]	1000	2000	3000	4000	5000
5	0.18 J/cm^2	0.18 J/cm^2	0.27 J/cm^2	0.25 J/cm^2	0.47 J/cm^2
10	0.27 J/cm^2	0.42 J/cm^2	0.49 J/cm^2	0.72 J/cm^2	1.25 J/cm^2
15	0.57 J/cm^2	0.66 J/cm^2	1.42 J/cm^2	1.35 J/cm^2	1.63 J/cm^2
20	0.41 J/cm^2	0.93 J/cm^2	1.32 J/cm^2	1.84 J/cm^2	2.59 J/cm^2
25	0.56 J/cm^2	1.37 J/cm^2	1.69 J/cm^2	2.04 J/cm^2	3.05 J/cm^2
30	0.67 J/cm^2	1.60 J/cm^2	2.00 J/cm^2	3.25 J/cm^2	3.80 J/cm^2

Point robot end-effectors impact energy densities were calculated and are presented in Tab. 1. Maximal energy densities were reached at highest deceleration (5000 mm/s^2) and at the stop point depth of 30 mm.
In literature the tolerance values were published regarding energy density of the impact and corresponding injury. Tissue injuries occur at the impact energy density higher than 2.52 J/cm^2, while hematoma or suffusion already occur below this value (Haddadin S., 2007b). Point impact energy densities that surpass the safe energy density limit are painted red in Tab. 1. The experimental results with our PMLA reveal that point impact can beside suffusion and hematoma cause serious tissue injury.

4. Conclusion

We have presented a human-robot impact emulation system and the preliminary tests conducted with the PMLA. Experiments were performed using point robot end-effector tool. In the experiments the robot end-effector collided with the PMLA perpendicularly at constant decelerations. The injury probability was evaluated by calculating the impact energy density.

In future, investigation with human volunteers will be carried out applying only safe robot impacts in order to verify the properties of our PMLA model.

5. References

Haddadin S., Albu-Schäffer A., Hirzinger G. 2007, Safety Evaluation of Physical Human-Robot Interaction via Crash-Testing, *Robotics: Science and Systems Conference (RSS2007)*, Atlanta, USA.

Haddadin S., Albu-Schäffer A., Hirzinger G. 2007, Safe Physical Human-Robot Interaction: Measurements, Analysis & New Insights, in *International Symposium on Robotics Research (ISRR2007), Hiroshima, Japan*.

Haddadin S., Albu-Schäffer A., Hirzinger G. 2008, The Role of the Robot Mass and Velocity in Physical Human-Robot Interaction – Part I: Unconstrained Blunt Impacts, *IEEE International Conference on Robotics and Automation (ICRA2008), pp. 1331-1338,* Pasadena, USA.

Haddadin S., Albu-Schäffer A., Hirzinger G. 2008, The Role of the Robot Mass and Velocity in Physical Human-Robot Interaction - Part II: Constrained Blunt Impacts, *IEEE International Conference on Robotics and Automation (ICRA2008), pp. 1339-1345,* Pasadena, USA.

Haddadin S., Albu-Schäffer A., Hirzinger G. 2008, Evaluation of Collision Detection and Reaction for a Human-Friendly Robot on Biological Tissues, *IARP International Workshop on Technical challenges and for dependable robots in Human environments*, Pasadena, USA.

Heinzmann J. and Zelinsky A. 2003, Quantitative Safety Guarantees for Physical Human-Robot Interaction, *Int. J. of Robotics Research*,vol. 22, no. 7-8, pp. 479–504.

Ikuta K., Ishii H., and Nokata M. 2003, Safety Evaluation Method of Design and Control for Human-Care Robots, *Int. J. of Robotics Research*, vol. 22, no. 5, pp. 281–298.

Klopčar N., Tomšič M., Lenarčič J. 2007, A Kinematic Model of Shoulder Complex to Evaluate the Arm-Reachable Workspace, *Journal of Biomechanics*, vol. 40, pp. 86-91.

Lim H.-O. and Tanie K. 2000, Human Safety Mechanisms of Human-Friendly Robots: Passive Viscoelastic Trunk and Passively Movable Base, *Int. J. of Robotics Research*, vol. 19, no. 4, pp. 307–335.

Acknowledgements This work was supported in part by the European Union. "Operation part financed by the European Union, European Social Fund."